

Ferromagnetic relaxation in $(\text{Ni}_{81}\text{Fe}_{19})_{1-x}\text{Cu}_x$ thin films: Band filling at high Z

Y. Guan^{a)} and W. E. Bailey

Materials Science Program, Department of Applied Physics, Columbia University, New York, New York 10027

(Presented on 8 January 2007; received 31 October 2006; accepted 22 November 2006; published online 4 April 2007)

We measure the compositional dependence of ferromagnetic relaxation (damping) in $(\text{Ni}_{81}\text{Fe}_{19})_{1-x}\text{Cu}_x$ magnetic thin films. The compositions tested ($0 \leq x \leq 0.30$) cover the decreasing, high- Z ($27.6 \leq Z \leq 28.0$) branch of the Slater-Pauling curve. Broadband (0–18 GHz) ferromagnetic resonance measurements in parallel (in-plane) and perpendicular (out-of-plane) resonance configurations reveal purely intrinsic, Gilbert-type damping, increasing with Cu content, from $\alpha = 0.0081 \pm 0.0003$ (no Cu) to $\alpha = 0.0242 \pm 0.0006$ (30% Cu). Despite the marked decrease in saturation magnetization $\mu_0 M_s$, in good agreement with Slater-Pauling values, the relaxation rate G also increases, from $G = 112 \pm 4$ MHz (no Cu) to $G = 150 \pm 4$ MHz (30% Cu). The results are similar in variation with Z to those found on the low- Z branch of the Slater-Pauling curve, in epitaxial $\text{Fe}_{1-x}\text{V}_x$. © 2007 American Institute of Physics. [DOI: [10.1063/1.2709750](https://doi.org/10.1063/1.2709750)]

I. INTRODUCTION

Ferromagnetic relaxation, or damping, is the physical process through which precessional (gigahertz) magnetization motion comes to a stop. The Landau-Lifshitz-Gilbert relaxation rate G directly controls the performance of gigahertz magnetic devices: critical currents i_{crit} in spin momentum transfer (SMT) switching¹ and frequency-swept linewidths for microwave absorption.^{2,3} Nevertheless, relaxation is not well understood, or characterized; values of intrinsic relaxation rate G have not been measured in many binary or ternary alloy systems of interest. Characterization of G across alloy systems can lead to an improved understanding of relaxation, as well as its more effective materials-based control.

$(\text{Ni}_{81}\text{Fe}_{19})_{1-x}\text{Cu}_x$ thin films have been of interest in their own right for use in SMT devices.^{4,5} The deliberate introduction of Cu into $\text{Ni}_{81}\text{Fe}_{19}$, reducing the moment, has made it much easier to magnetize one film normal to the plane with attainable fields $B_{\perp} < 1$ T. SMT efficiencies are known to be larger where magnetization directions of \mathbf{M}_1 , \mathbf{M}_2 are perpendicular to each other.

The composition range spanned by $(\text{Ni}_{81}\text{Fe}_{19})_{1-x}\text{Cu}_x$ can address a leading theory of ferromagnetic damping. Kambersky^{6,7} has proposed a dependence of ferromagnetic relaxation rate G (damping α) on effective g factor (g_{eff}) as $G \propto (g_{\text{eff}} - 2)^2 (a\tau + b\tau^{-1})$, where τ denotes the scattering time, and pure spin type magnetism is expected as $g_{\text{eff}} = 2$. According to the magnetomechanical measurements of Barnett,^{8,9} g_{eff} follows a rough compositional dependence, similar to the Slater-Pauling curve, but peaked at $Z = 27$ (Co). Decreasing values in g_{eff} may thus be expected in $(\text{Ni}_{81}\text{Fe}_{19})_{1-x}\text{Cu}_x$ thin films with increasing Cu content, if thin film results are simi-

lar to those seen in bulk crystals; according to the Kambersky theory,^{6,7} reduced values in g_{eff} may produce reduced values in G .

In this article, we present a detailed ferromagnetic resonance and relaxation (damping) of $(\text{Ni}_{81}\text{Fe}_{19})_{1-x}\text{Cu}_x$ thin films. We found that the saturation magnetization and relaxation rate (damping) can be effectively controlled by means of Cu content in thin $\text{Ni}_{81}\text{Fe}_{19}$ films.

II. EXPERIMENT

Alloys of $(\text{Ni}_{81}\text{Fe}_{19})_{1-x}\text{Cu}_x$ (50 nm) thin films were grown onto Si/SiO₂ substrates using UHV magnetron sputtering at a base pressure of 4×10^{-9} Torr. $(\text{Ni}_{81}\text{Fe}_{19})_{1-x}\text{Cu}_x$ samples were made by confocal sputtering from $\text{Ni}_{81}\text{Fe}_{19}$ alloy and elemental Cu targets under an applied deposition field of 20 Oe.

Cu doped $\text{Ni}_{81}\text{Fe}_{19}$ alloy thin films (50 nm thick), with doping levels of 0%, 20%, and 30%, were investigated in the study. All these films were capped with a sputtered 5 nm Cu layer to prevent oxidation before transport to air. Atomic fluxes of each source to the substrate, operating separately, were calibrated using a quartz crystal monitor, located in front of the substrate position, immediately prior to film deposition. Rates for each alloy composition were subsequently calibrated using the atomic force microscopy (AFM).

The Cu doped $\text{Ni}_{81}\text{Fe}_{19}$ (50 nm) thin films were characterized using broadband (0–18 GHz) ferromagnetic resonance (FMR) measurements in parallel (in-plane) and perpendicular (out-of-plane) resonance configurations. All measurements were carried out at room temperature. More details about broadband FMR setup and measurement technique can be found in our previous work.¹⁰

^{a)}Electronic mail: yg2111@columbia.edu

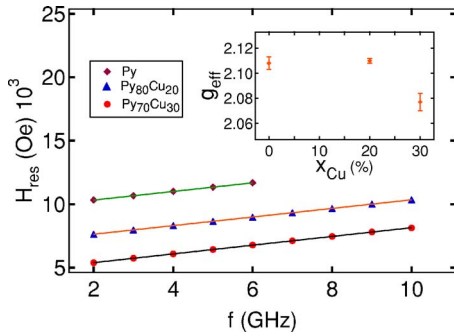


FIG. 1. (Color online) Variable-frequency out-of-plane resonance fields $H_{\text{res}}(\omega)$ of $\text{Ni}_{81}\text{Fe}_{19}$ films with different Cu doping. Solid lines are linear fits to Eq. (1). The inset shows the effective g factors g_{eff} extracted from the slope of the linear fits.

III. RESULTS AND DISCUSSION

The resonant field H_{res} and the linewidth ΔH_{pp} were measured through conventional broadband FMR over the range of 2–10 GHz for out-of-plane and 2–16 GHz for in-plane measurements.

For out-of-plane FMR measurements, the Kittel relationship between applied bias field H and FMR frequency f can be written as (surface anisotropy is neglected)¹¹

$$\omega = \mu_0 \gamma_0 g_{\text{eff}} (H - M_s), \quad (1)$$

where $\gamma_0 g_{\text{eff}}$ is the effective gyromagnetic ratio, 175.8 GHz/T for $g_{\text{eff}}=2$.

Plots of out-of-plane resonant field H_{res} as a function of resonant frequency, with linear fits to Eq. (1), are shown in Fig. 1 for all samples. Fits to this equation yield independent measurements of g_{eff} (slope) and $\mu_0 M_s$ (intercept). The extracted effective g factors (g_{eff}) change from 2.10 ± 0.01 for pure $\text{Ni}_{81}\text{Fe}_{19}$ to 2.07 ± 0.01 for 30% Cu doped $\text{Ni}_{81}\text{Fe}_{19}$. With increasing doping levels, the saturation magnetization ($\mu_0 M_s$) values decrease clearly, from 0.965 T for pure $\text{Ni}_{81}\text{Fe}_{19}$ to 0.471 T for 30% Cu doped $\text{Ni}_{81}\text{Fe}_{19}$.

For in-plane FMR measurements, the Kittel relationship between applied bias field H and FMR frequency f has been used to estimate saturation magnetization $\mu_0 M_s$ and anisotropy field H_k in the films, written as¹¹

$$\omega = \mu_0 \gamma_0 g_{\text{eff}} \sqrt{(H + H_k + M_s)(H + H_k)}. \quad (2)$$

Plots of square of resonant frequency f^2 as a function of in-plane resonant field H_{res} are shown in Fig. 2 for all

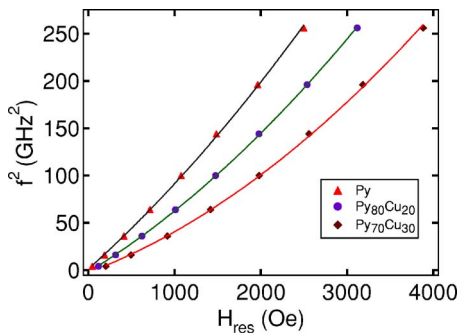


FIG. 2. (Color online) In-plane Kittel plot of $\text{Ni}_{81}\text{Fe}_{19}$ films with different Cu doping. Solid lines are nonlinear fits to Eq. (2).

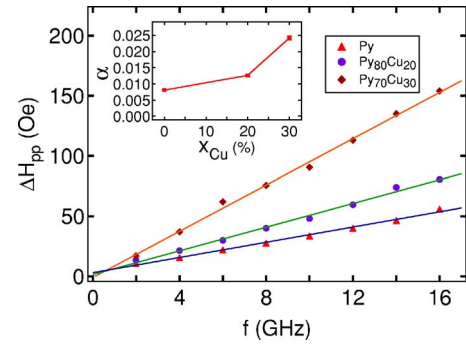


FIG. 3. (Color online) Variable-frequency in-plane linewidths $\Delta H_{\text{pp}}(\omega)$ of $\text{Ni}_{81}\text{Fe}_{19}$ films with different Cu doping. Solid lines are linear fits to Eq. (3). The inset shows the damping constant α extracted from the slope of the linear fits.

samples. The nonlinear fits to Eq. (2), using $\mu_0 M_s$ and H_k as free parameters and g_{eff} from out-of-plane FMR measurements, are included. The extracted saturation magnetization values decrease with increasing doping levels of Py films, from 0.934 T for pure $\text{Ni}_{81}\text{Fe}_{19}$ to 0.426 T for 30% Cu doped $\text{Ni}_{81}\text{Fe}_{19}$, shown in Fig. 4, very close to those extracted values from out-of-plane measurements.

Damping constants α can be obtained through the field-swept linewidth ΔH_{pp} of variable-frequency in-plane FMR measurements, according to

$$\mu_0 \Delta H_{\text{pp}} = \mu_0 \Delta H_0 + \frac{2}{\sqrt{3}} \frac{\alpha \omega}{\gamma_0 g_{\text{eff}}}, \quad (3)$$

where linewidth can be divided between homogeneous and inhomogeneous types.¹²

Homogeneous linewidth is proportional to resonant frequency, described by the Landau-Lifshitz-Gilbert (LLG) damping parameter α (dimensionless) or relaxation rate G (megahertz).¹³ Inhomogeneous linewidth is independent of resonant frequency, described by ΔH_0 , arising from a locally inhomogeneity of microstructure.

The variable-frequency in-plane FMR linewidths $\Delta H_{\text{pp}}(\omega)$ are shown in Fig. 3, with linear fits to Eq. (3), for all samples. Using the effective g factors (g_{eff}) from out-of-plane FMR measurements, damping constants α can be extracted, shown in the inset of Fig. 3. There is a clear increase in slope with increasing Cu doping, where α values increase from 0.0081 ± 0.0003 for pure $\text{Ni}_{81}\text{Fe}_{19}$ to 0.0242 ± 0.0006 for 30% Cu doped $\text{Ni}_{81}\text{Fe}_{19}$.

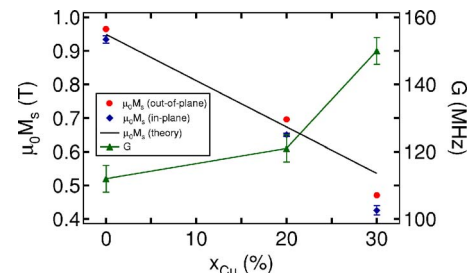


FIG. 4. (Color online) Saturation magnetization $\mu_0 M_s$ of various Cu doping $\text{Ni}_{81}\text{Fe}_{19}$ films extracted from both out-of-plane and in-plane broadband FMR measurements, including the comparison with theoretical calculation. Extracted LLG relaxation rates G are also shown here.

The extracted values of saturation magnetization from broadband FMR measurements are compared with theoretical values based on the well-known Slater-Pauling relation¹⁴

$$\mu_0 M_s(x_{\text{Cu}}) \cong \mu_0 M_s(x_{\text{Cu}} = 0) - 1.38x_{\text{Cu}}(T), \quad (4)$$

where x_{Cu} denotes the concentration of Cu doping in $\text{Ni}_{81}\text{Fe}_{19}$ films. In the calculation, we take the theoretical value of zero doping $\text{Ni}_{81}\text{Fe}_{19}$ film as the average of those two extracted values from out-of-plane and in-plane FMR measurements. As shown in Fig. 4, the extracted values from broadband FMR measurements are consistent with the theoretical values. The results are also similar in variation with Z to those found on the low- Z branch of the Slater-Pauling curve, in epitaxial $\text{Fe}_{1-x}\text{V}_x$.¹⁵ LLG relaxation rate G can be related to damping parameter α by

$$G^{\text{cgs}} = G^{\text{SI}}/4\pi = \mu_0 M_s \gamma_0 g_{\text{eff}} \alpha / 4\pi. \quad (5)$$

Using $\mu_0 M_s$ and α from in-plane FMR measurements and g_{eff} from out-of-plane FMR measurements, G values can thus be obtained according to Eq. (5). As shown in Fig. 4, when Cu is alloyed into $\text{Ni}_{81}\text{Fe}_{19}$, G increases despite the decrease of saturation magnetization, from 112 ± 4 MHz for pure $\text{Ni}_{81}\text{Fe}_{19}$ to 150 ± 4 MHz for 30% Cu doped $\text{Ni}_{81}\text{Fe}_{19}$.

The LLG relaxation rates G as a function of Cu content extracted from our broadband FMR measurements do not follow a simple dependence on the effective g factor g_{eff} , which poses some interesting questions about the fundamental nature of relaxation. It is not obvious that the Kambersky theory^{6,7} holds here, as the $g_{\text{eff}} - 2$ does not increase as Cu is added, but vibrates within the small range of 2.11–2.07. A further electrical measurement of the scattering time τ is thus needed to test the Kambersky theory for Cu doped $\text{Ni}_{81}\text{Fe}_{19}$ samples.

IV. CONCLUSION

Ferromagnetic resonance and relaxation (damping) of $(\text{Ni}_{81}\text{Fe}_{19})_{1-x}\text{Cu}_x$ thin films have been measured by broadband FMR technique in parallel (in-plane) and perpendicular (out-of-plane) resonance configurations. It is found that the saturation magnetization $\mu_0 M_s$ decreases with increasing Cu doping concentration, in good agreement with Slater-Pauling values. In addition, the LLG damping constant α and relaxation rate G both increase with more Cu alloyed into $\text{Ni}_{81}\text{Fe}_{19}$ despite the marked decrease of moment.

ACKNOWLEDGMENTS

This work was supported by the Army Research Office with Grant No. ARO-43986-MS-YIP and the National Science Foundation with Grant No. NSF-DMR-02-39724.

- ¹J. C. Slonczewski, *J. Magn. Magn. Mater.* **159**, L1 (1996).
- ²C. Scheck, L. Cheng, and W. E. Bailey, *Appl. Phys. Lett.* **88**, 252510 (2006).
- ³C. E. Patton, *J. Appl. Phys.* **39**, 3060 (1968).
- ⁴P. M. Braganca, I. N. Krivorotov, O. Ozatay, A. G. F. Garcia, N. C. Emley, J. C. Sankey, D. C. Ralph, and R. A. Buhrman, *Appl. Phys. Lett.* **87**, 112507 (2005).
- ⁵J. C. Sankey, P. M. Braganca, A. G. F. Garcia, I. N. Krivorotov, R. A. Buhrman, and D. C. Ralph, *Phys. Rev. Lett.* **96**, 227601 (2006).
- ⁶V. Kamberský, *Can. J. Phys.* **48**, 2906 (1970).
- ⁷J. Kuneš and V. Kamberský, *Phys. Rev. B* **65**, 212411 (2002).
- ⁸R. M. Bozorth, *Ferromagnetism* (Van Nostrand, New York, 1951), p. 453.
- ⁹S. J. Barnett, *Rev. Mod. Phys.* **7**, 129 (1935).
- ¹⁰V. Dasgupta, N. Litombe, and W. E. Bailey, *J. Appl. Phys.* **99**, 08G312 (2006).
- ¹¹C. Kittel, *Introduction to Solid State Physics* (Wiley, New York, 2005), p. 381.
- ¹²B. Heinrich, in *Ultrathin Magnetic Structures II* edited by B. Heinrich and J. A. C. Bland (Springer-Verlag, Berlin, 1994), Chap. 3, pp. 195–222.
- ¹³L. D. Landau, E. M. Lifshitz, and L. P. Pitaevski, *Statistical Physics* (Pergamon, Oxford, 1980), Pt. 2.
- ¹⁴R. C. O'Handley, *Modern Magnetic Materials: Principles and Applications* (Wiley, New York, 2000), Chap. 5, pp. 144–150.
- ¹⁵C. Scheck, L. Cheng, I. Barsukov, Z. Frait, and W. E. Bailey, *Phys. Rev. Lett.* (in press).